JOURNAL OF COMPUTATIONAL PHYSICS 100, 306–321 (1992)

A Numerical Study of a Rotationally Degenerate Hyperbolic System. Part I. The Riemann Problem

HEINRICH FREISTÜHLER

Institut für Mathematik, RWTH Aachen, D-5100 Aachen, Germany

AND

E. BRUCE PITMAN*

Department of Mathematics, State University of New York, Buffalo, New York 14214

Received August 21, 1990; revised July 22, 1991

We study numerically the Riemann problem for a 2 × 2 system of conservation laws with a cubic flux function, a particular case of the class of models introduced by Keyfitz and Kranzer. The system is not strictly hyperbolic, and the classical Lax theory for hyperbolic systems is not directly applicable. Correspondingly, some numerical schemes which are accurate for strictly hyperbolic systems are not well behaved for this example. When they do work, different schemes yield markedly different results for certain data. We explain this effect by observing that, near these data, viscous regularization is non-uniform as the viscosity tends to zero. This fact does not contradict the well-posedness of the hyperbolic model; it does imply that precise control of the viscosity introduced into a computational method is crucial for generating the correct numerical solutions. We examine all of these issues and comment on their implications for similar systems which arise in continuum mechanics.

1. INTRODUCTION

Consider the system of hyperbolic conservation laws given by

$$U_t + (|U|^2 U)_x = 0, \tag{1.1}$$

where $U = (u, v) \in \mathbb{R}^2$. This system is not strictly hyperbolic, since the two eigenvalues of the Jacobian $D(|U|^2 U)$, viz. $\lambda^r(U) = 3|U|^2$ and $\lambda^a(U) = |U|^2$, are equal at the origin $U = 0$. Away from $U = 0$, the fast radial mode (corresponding to λ^r, eigenvector (u, v)) is genuinely non-linear in the sense of Lax [30], while the slow angular mode (corresponding to λ^a, eigenvector $(v, -u)$) is linearly degenerate.

* Supported by the Air Force Office of Scientific Research under Grant AFOSR 900076.

The present article is the first in a planned series of three papers [17, 18] in which we study the system (1.1) numerically. In this Part I we restrict attention to the Riemann problem. The Riemann problem consists of finding a (weak) solution of (1.1) which assumes the initial values

$$U(x, 0) = U^0(x) = \begin{cases} U_l, & x < 0 \\ U_r, & x > 0. \end{cases} \tag{1.2}$$

For purposes of our discussion, it is helpful to consider polar coordinates in phase space, i.e., $r: \mathbb{R}^2 \to [0, \infty)$, $\theta: \mathbb{R}^2 \to \mathbb{R} \bmod 2\pi$ defined by $U = r(U)(\cos(\theta(U)), \sin(\theta(U))$. An intuitively plausible way to assign a centered, piecewise continuous solution to (1.1)–(1.2) is to combine (i) a contact discontinuity in the slow family, which rotates the state variables from U_l to an intermediate state U_m, where $r(U_l) = r(U_m)$, with (ii) a shock or rarefaction wave from U_m to U_r, along which $\theta = \text{const}$ (see [12]).

For comparison, consider also the reduced system obtained by setting $v \equiv 0$ in (1.1):

$$u_t + (u^3)_x = 0. \tag{1.3}$$

The Riemann problem for this scalar equation may be solved by following the construction of Liu [32] and Wendroff [45] for non-convex flux functions. In addition to the "classical" solutions to (1.2) consisting of either a single shock or rarefaction wave, the non-convexity of (1.2) introduces composite wave solutions, consisting of a shock juxtaposed with a rarefaction. Of course, completing such a scalar solution with a v-component which is identically equal to zero gives solutions to the full problem for special, co-linear data.

0021-9991/92 $5.00

These two constructions suggest a non-uniqueness of solutions and/or a non-continuous dependence of the solutions on initial data. In order to illustrate this difficulty, consider the Riemann problem (1.1)–(1.2) with data

$$U_l = (1, 0), \qquad U_r = (\cos \delta, \sin \delta) \tag{1.4}$$

for values of δ near π. If $\delta = \pi$ exactly, the two constructions yield two different solutions. One solution consists of a contact discontinuity joining U_l to U_r; the other solution is composed of a shock joining U_l to a middle state $U_c = (-\frac{1}{2}, 0)$ and an adjacent rarefaction wave joining U_c to U_r. In both solutions, $v \equiv 0$. The composite wave solution, being the solution of a restricted problem, might seem more natural. On the other hand, the contact wave solution may readily be extended to data (1.4) with $\delta \neq \pi$. The continuity of the contact wave solution operator, as data moves off of the line $v = 0$, seems a desirable property. Indeed, as long as δ is different from π, there is no centered, piecewise smooth solution of (1.1)–(1.4) which would, in the limit $\delta \to \pi$, approach the composite wave solution. Conversely, any contact discontinuity is the limit of smooth, quasistationary solutions of (1.1).

Our present study aims at describing how the system (1.1) can be treated numerically, in a consistent and justifiable way. Because the system is strictly hyperbolic except at one point, one might hope that standard numerical methods will work adequately in local regions which do not contain the umbilic point; it is less clear how such methods might work near the umbilic point, or for large data "surrounding" it. Indeed, we will show that different numerical methods yield markedly different results for certain special data. This differing of computational results is related to the potential multiciplicity of solutions discussed in the previous paragraph and is intimately connected with a non-uniformity of the classical vanishing viscosity approach (cf. Freistühler [13, 14, 16] and Liu [35]). *Regarding solutions of the parabolic regularization* $U_t + (|U|^2 U)_x = \varepsilon U_{xx}$ of (1.1), *the following statement holds for certain data: For each fixed positive value of the viscosity coefficient* ε, *the solution is stable against perturbations of the initial data, but the region of stability shrinks to zero as* $\varepsilon \searrow 0$. This result suggests that the classical tool of artificial viscosity should not be employed on rotationally degenerate systems without exercising great caution. Regarding numerical methods, we emphasize that precise control over the size of any numerical viscosity is indispensable in these special cases.

A major motivation to study model (1.1) is its rôle as a prototype of larger systems which arise in continuum mechanics (see [12]). There is a precise isomorphism between the wave pattern of (1.1) and (the transverse) part of the wave pattern of any generic rotationally degenerate system of hyperbolic conservation laws [11, 12]. Systems which describe plane wave propagation of isotropic, multi-dimensional systems are rotationally degenerate [11]. Recently, Brio and Hunter [4] have derived (1.1) from larger continuum mechanics models by formal asymptotic techniques.

Two particular areas of continuum mechanics to which these comments apply are magnetohydrodynamics and isotropic elasticity. In the case of magnetohydrodynamics, (1.1) was derived long ago by Cohen and Kulsrud [7], who used it to explain specific features of the solar wind. The Riemann problem for the full MHD system was treated analytically by Gogosov [23], and computational results have been presented by Brio and Wu [5] and Wu [46]. In related work, recent computations for (1.1) were presented in [27]. Keyfitz and Kranzer [28] and Shearer [42] studied the Riemann problem for a thin elastic string, and Fehribach and Shearer [10], Gilquin and Serre [19], and Tait [43] have performed computations on this problem. The paper [11] addresses both MHD and elasticity. The systematic numerical study of (1.1) which we present here continues the analytic work of [11, 12, 14].

We conclude this introduction by outlining the format for the rest of this paper. Section 2 describes the computational methods employed in this study, and Section 3 presents numerical results. Section 4 interprets these results and returns to our discussion of how (1.1) relates to more realistic continuum mechanics models.

2. COMPUTATIONAL METHODS

In this section, we discuss issues pertinent to the numerical computation of solutions to (1.1). After reviewing some fundamental ideas and results in the theory of (strictly) hyperbolic conservation laws in Sub-section 2.1, in Sub-sections 2.2 through 2.4 we give a brief introduction to numerical methods for such systems. We address the issue of non-strict hyperbolicity in Sub-section 2.5. Finally, in 2.6 we comment on the numerical schemes we use in our study.

Sub-sections 2.1 through 2.4 are not intended to give a complete review of the theory of numerical schemes for hyperbolic systems of conservation laws; for this purpose, we refer the reader to the paper of Harten, Lax, and van Leer [24]. Here we restrict ourselves to those basic ideas which we need in order to explain our selection of computational schemes and to have sufficient background for discussing the numerical results. On the other hand, the scope of this section is broader than one would need for the Riemann problem alone; it is meant to establish a basis for the whole of our study, including [17, 18]. Thus the relationship between this section and the rest of this paper is that a number of general issues are raised here, and are further addressed in the other sections within the relatively simple framework of the Riemann problem for (1.1).

2.1. *Introductory Theory*

In this sub-section we review some of the basic facts about hyperbolic systems of conservation laws. Such systems are of the general form

$$w_t + (f(w))_x = 0, \qquad w(x, 0) = w^0(x), \tag{2.1}$$

where and f: $\mathbb{R}^m \to \mathbb{R}^m$ and $x, t \in \mathbb{R}$. (2.1) is called hyperbolic if the Jacobian Df of the flux function is diagonalizable over $\mathbb{R}$; of particular importance is the case of strict hyperbolicity, when all the eigenvalues of Df are distinct.

It is known that smooth solutions of (2.1) typically break down after finite time. Therefore one considers weak solutions, i.e., functions w which satisfy (2.1) in the sense of distributions,

$$\int_0^\infty \int_{-\infty}^\infty (\varphi_t(x, t)\, w(x, t) + \varphi_x(x, t) f(w(x, t)))\, dx\, dt + \int_{-\infty}^\infty \varphi(x, 0)\, w^0(x)\, dx = 0, \tag{2.2}$$

for all $\varphi \in C^\infty(\mathbb{R}^2, \mathbb{R})$ with compact support. Across any curve of discontinuity, (2.2) enforces the Rankine–Hugoniot conditions:

$$C(w^+ - w^-) = f(w^+) - f(w^-). \tag{2.3}$$

Here, C is the propagation speed of the discontinuity and w^-, w^+ indicate the states just to the left and right of the discontinuity. (These notions are due to Lax [30].) For strictly hyperbolic systems, Glimm [20] proved the existence of weak solutions for initial data of small total variation; a later extension is due to Liu [34]. Unfortunately, weak solutions of (2.1) are not uniquely determined by the initial data, and a selection principle is required to choose the physically relevant solution. For strictly hyperbolic systems, this selection problem may be considered as resolved in a satisfactory manner. In the case of scalar conservation laws ($m = 1$), the vanishing viscosity approach has been carried out completely (see [29, 30, 38]). For arbitrary measurable initial data a unique solution may be obtained as the limit, when $\varepsilon \searrow 0$, of the viscous regularization

$$w_t + (f(w))_x = \varepsilon w_{xx}; \tag{2.4}$$

this viscosity solution depends $\mathscr{L}^1_{\text{loc}}$-continuously on the data. When this solution is piecewise smooth (which is a generic property [40]), it may be characterized by an explicit admissibility criterion which must be satisfied pointwise at discontinuities, namely the entropy condition of Lax [30] or that of Oleinik [38].

These entropy conditions carry over to strictly hyperbolic systems (see Lax [30] and Liu [32]). While convergence of the viscosity method for general strictly hyperbolic systems is still an open question, Lax's and Liu's conditions have been shown to be equivalent, for small amplitude quasi-stationary step discontinuities, to the existence of viscous profiles, i.e., traveling wave solutions of (2.4) which approximate these quasi-stationary discontinuities as $\varepsilon \downarrow 0$ [37]. For initial data with small variation, the Riemann problem for a strictly hyperbolic system has a unique, self-similar, piecewise continuous solution satisfying the Lax–Liu entropy conditions [30, 32], consisting of constant states joined by shock and rarefaction waves. (For certain specific systems of conservation laws, analogous results have been proved for arbitrary initial data.)

These ideas have been applied in the development of numerical schemes for (2.1). However, they do not necessarily carry over to non-strictly hyperbolic systems.

2.2. *Conservative and Upwind Differencing*

In order to describe numerical schemes for (2.1), discretize (a finite interval of) space into N small intervals of equal length Δx and time into discrete steps Δt. Assume we know w at space points $i\,\Delta x$, $i \in 1, \ldots, N+1$, at time $n\,\Delta t$. We write

$$w_i^n = w(i\,\Delta x, n\,\Delta t), \qquad f_i^n = f(w_i^n),$$

and ask how to advance w^n to w^{n+1}.

Equation (2.1) describes the conservation of a field variable w whose flux is $f(w)$; we mimic this conservation principle by considering conservative numerical schemes. A conservative scheme in which w_i^{n+1} depends only on the three values w_{i-1}^n, w_i^n, w_{i+1}^n may be written as a numerical flux difference

$$w_i^{n+1} = w_i^n - \frac{\Delta t}{\Delta x}\,(g(w_{i+1}^n, w_i^n) - g(w_i^n, w_{i-1}^n)). \tag{2.5}$$

Here, the time step Δt must be restricted by the Courant–Friedrichs–Lewy condition, which states $a\,\Delta t/\Delta x \leqslant 1$, where a is the maximum of the (absolute value of the) eigenvalues of Df. The function $g(\cdot, \cdot)$ is called the numerical flux, and must be consistent with the physical flux $f(\cdot)$ in the sense that

$$g(w, w) = f(w).$$

The simplest scheme one might think of trying would be to approximate (2.1) by difference quotients in time and space, with the spatial differentiation following the characteristics of the system, i.e., upwind differencing. For (1.1),

where characteristic speeds are always non-negative, upwinding gives

$$w_i^{n+1} = w_i^n - \frac{\Delta t}{\Delta x}(f_i^n - f_{i-1}^n). \tag{2.6}$$

Note that upwind differencing is conservative, with a numerical flux

$$g(w_{i+1}, w_i) = f(w_i).$$

The difference scheme (2.6) is of first-order accuracy (for smooth solutions). The behavior of this scheme near discontinuities will be addressed in Sub-section 2.4.

2.3. *Godunov and Random Choice Schemes*

Many modern schemes for solving hyperbolic systems (2.1) are based on explicitly resolving the local wave dynamics defined by (2.1), accounting for the nonlinearity of f and possible discontinuities in the solution. These schemes have their origins in the method introduced by Godunov [22]. To describe Godunov's method, consider an approximation $\bar{w}_i^0$ of the initial data $w^0(x)$, constant over each cell $(i-\frac{1}{2})\Delta x < x < (i+\frac{1}{2})\Delta x$. At each cell edge, there is a (possible) discontinuity in $\bar{w}^0$, and one must solve a Riemann problem locally. Restrict the timestep $\Delta t < \Delta x/2a$, so that waves from adjacent Riemann problems do not interact. For $0 \leqslant t \leqslant \Delta t$ consider the exact solution to (2.1), composed of the solutions to all of these local Riemann problems. Define w^1 as the restriction of this solution to the line $t = \Delta t$. Now find a piecewise constant approximation $\bar{w}^1$ to w^1, which will in turn serve as data for advancing the solution from $t = \Delta t$ to $t = 2\Delta t$. Continue in this manner to find w^{n+1} and $\bar{w}^{n+1}$, with w^{n+1} the restriction of an exact solution (defined on the strip $n\Delta t \leqslant t \leqslant (n+1)\Delta t$ by data $\bar{w}^n$ at $t = n\Delta t$) to $t = (n+1)\Delta t$, and $\bar{w}^{n+1}$ its piecewise constant approximation.

Different numerical schemes may be obtained by altering the ansatz for solving the local Riemann problems and for obtaining $\bar{w}^n$ from w^n. Godunov obtained his approximation by solving each Riemann problem exactly and then averaging w^{n+1} over each cell $((i-\frac{1}{2})\Delta x, (i+\frac{1}{2})\Delta x)$. We remark that Godunov's method may be put in conservative form [24].

In his existence proof [20], Glimm proposed an alternative procedure for obtaining $\bar{w}_i^{n+1}$. Instead of averaging over the computational cells, Glimm samples the Riemann solution at one point in each cell. Providing the sampling points are uniformly distributed within every interval, then with probability one all waves will be correctly described. Glimm's original proposal was to randomly sample the interval; Liu [33] showed that equidistributed sampling is sufficient for the existence proof. This random choice construction was later developed into a method for numerical computations; for references, see Colella [8], who suggested using the equidistributed van der Corput sequence for the sampling strategy.

To implement a Godunov or random choice scheme, one must specify a procedure for solving a Riemann problem at each cell edge, for each time step. Solving all these local Riemann problems in a numerical scheme is, in general, an expensive process. Moreover, only a limited amount of information from the exact solution is usually ever used (e.g., the average over subintervals in Godunov's scheme). Therefore, it is often advantageous to replace the exact Riemann solver with an approximate solver which preserves salient features of the solution. [24] describes the construction of approximation Riemann solvers.

The Godunov and random choice schemes, as we have described them above, are first-order accurate in space and time. Higher order modifications of the Godunov scheme have been developed, beginning with the work of van Leer [31]. These schemes attain high order accuracy in space by choosing the approximants $\bar{w}_i^n$ as a piecewise high order polynomial (often linear) instead of piecewise constant. High accuracy in time is usually achieved by a predictor–corrector methodology. These high order schemes must include certain "slope limiting" or "flux limiting" procedures to prevent the introduction of spurious extrema caused by the discrete representation of the solution. See [31] for details.

2.4. *Artificial Viscosity*

As remarked in Sub-section 2.1, an admissibility condition must be imposed in order to select a unique and physically meaningful weak solution of (2.1). In numerical schemes for strictly hyperbolic systems, a small viscosity is sufficient for this purpose. This viscosity is not usually added to (2.1) explicitly, but rather is introduced through the design of the scheme.

Consider, for example, the special case of upwinding for a linear, scalar conservation law $w_t + aw_x = 0$, with $a > 0$. It is easy to see that in this case (2.6) may be rewritten

$$w_i^{n+1} = w_i^n - \frac{a\Delta t}{2\Delta x}(w_{i+1}^n - w_{i-1}^n) + \frac{a\Delta t}{2\Delta x}(w_{i+1}^n - 2w_i^n + w_{i-1}^n). \tag{2.7}$$

The last term is a difference approximation to w_{xx}. Thus, scheme (2.6) may be viewed as solving, with second-order accuracy, the parabolic equation (2.4) with a viscosity coefficient

$$\varepsilon = \frac{a\Delta x}{2}\left(1 - \frac{a\Delta t}{\Delta x}\right). \tag{2.8}$$

The high order Godunov schemes incorporate a selective amount of artificial viscosity. In particular, near a large gradient the "limiter" reduces the spatial interpolation to zeroth order (i.e., constant), and the whole scheme essentially reverts to upwind differencing. We emphasize that this extra dose of viscosity is included only near large jumps in the data, such as found at a shock; away from sharp transitions, the limiters are turned off and the artificial viscosity is reduced. Indeed, it is precisely this well regulated inclusion of viscosity which gives the Godunov methods their high degree of resolution. For strictly hyperbolic systems, the utility of employing artificial viscosity in numerical calculations follows from the theoretical success of the vanishing viscosity approach.

By employing probabilistic sampling, the random choice method introduces no artificial viscosity. This allows for perfect shock resolution; that is, the width of the shock transition is zero. The question of admissibility is addressed in the analytic construction of the Riemann solver.

2.5. *Non-strictly Hyperbolic Systems*

When hyperbolicity is no longer strict, results are available only for special systems or classes of systems. In particular, for systems whose flux function is of the form $f(w)=\varphi(w)w$, existence results have been obtained via Glimm's construction by Liu and Wang [36] and Temple [44]. Such fluxes were introduced by Keyfitz and Kranzer [28], and include (1.1). Other results concerning the Riemann problem for special cases of non-strictly hyperbolic systems were derived by Isaacson [25], Shearer [42], Schaeffer, Shearer, Marchesin, and Paes-Leme [41], Isaacson, Marchesin, Plohr, and Temple [26], and Freistühler [11, 12].

A few attempts and suggestions have been made to apply some of the computational methods outlined above to non-strictly hyperbolic systems. For schemes which do not explicitly refer to the wave-curve geometry of the Riemann solution in phase space, such extensions are, in principle, direct. This has been done for MHD in [5]. For schemes which do refer to the wave-curve geometry, Bell, Colella, and Trangenstein [3] have suggested modifications of the high order Godunov methodology which account for the special character of this geometry near points in phase space where strict hyperbolicity is lost.

Speaking generally, when studying non-strictly hyperbolic systems numerically, the typical experience is to find that "the nature of the computationally resolved wave patterns depends sensitively on the choice of the numerical method" [21]. The lack of a general solution theory is no explanation for such inconsistency. Rather, the lack of theory and the computational sensitivity may have a common source. It is our contention that, because the vanishing viscosity approach is not well-behaved in general, incorporation of artificial viscosity in numerical schemes without careful reflection on the nature of the problem to be solved can lead to severe errors. One must make a clear distinction between solving the hyperbolic system (2.1) and the related parabolic regularization (2.4).

2.6. *Schemes Used in This Study*

In our study, we solved (1.1) using the random choice scheme, a simple upwind scheme, and two second-order Godunov-type schemes, that of Bell, Colella, and Trangenstein, [3] and that of Roe [39]. We also used a variant of the random choice method which integrates the viscous problem

$$U_t+(|U|^2\,U)_x=\varepsilon U_{xx}, \qquad \varepsilon>0; \tag{2.9}$$

this is done by fractional steps, first solving $U_t+(|U|^2\,U)_x=0$ by random choice, then using Crank–Nicholson to solve $U_t=\varepsilon U_{xx}$. (In fact, we used a Strang splitting, calling the random choice solver for time $\Delta t/2$, Crank–Nicholson for Δt, and finishing with another call to random choice for a half-step.) We view (2.9) as introducing a controlled amount of diffusion into the calculation and have compared the results obtained from this scheme for different values of ε with the results produced by the other methods.

The random choice method was coded using the "intuitive" centered wave construction introduced in Section 1 (see Section 4.1 for analytic results on this solution.) Following [8], we used the van der Corput sequence for the sampling strategy. Upwind differencing is completely defined by Eq. (2.6). The two second-order Godunov-type schemes are detailed in [3, 24, 39].

3. NUMERICAL RESULTS

Here we present the results from a series of numerical experiments, carried out for different initial data and with different schemes. In Section 4.2, we draw together these numerical findings by calling upon analytic results about (1.1).

FIG. 1. Results from the Random Choice and Godunov schemes for various values of ρ and δ, at time $T=0.75$. Shown are the plots of u(——) and v(– – –). We exhibit only the range $0\leqslant x\leqslant 3$ (neglecting the trivial piece $-0.15\leqslant x\leqslant 0$). In Figure 1.1, $\rho=0.25$ and δ takes the values 0.25π, 0.75π, 1.0π, as indicated on the top label. In Figure 1.2, $\rho=0.75$; Figure 1.3, $\rho=1.0$; Figure 1.4, $\rho=1.1$.

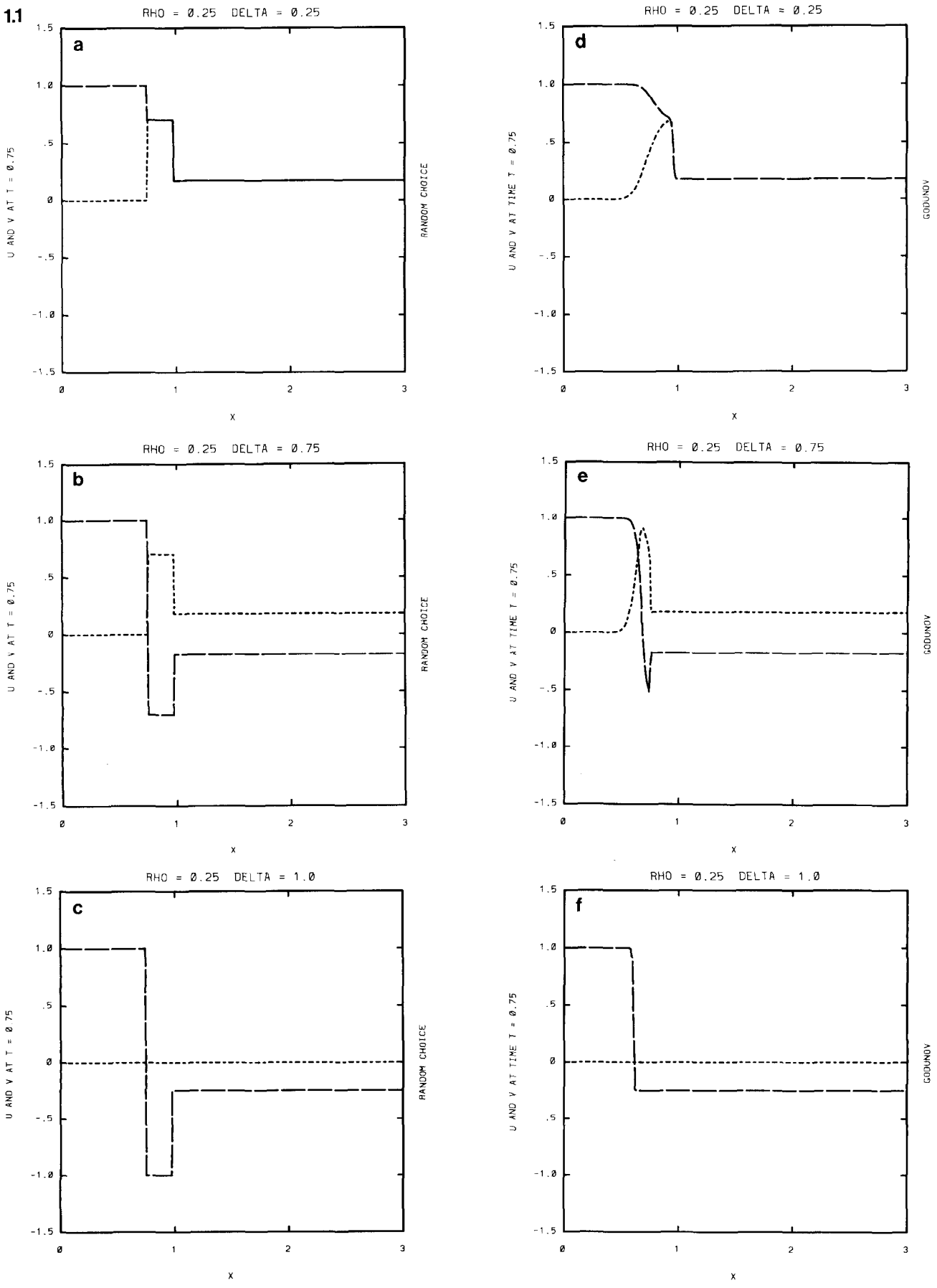

FIG. 1—*Continued*

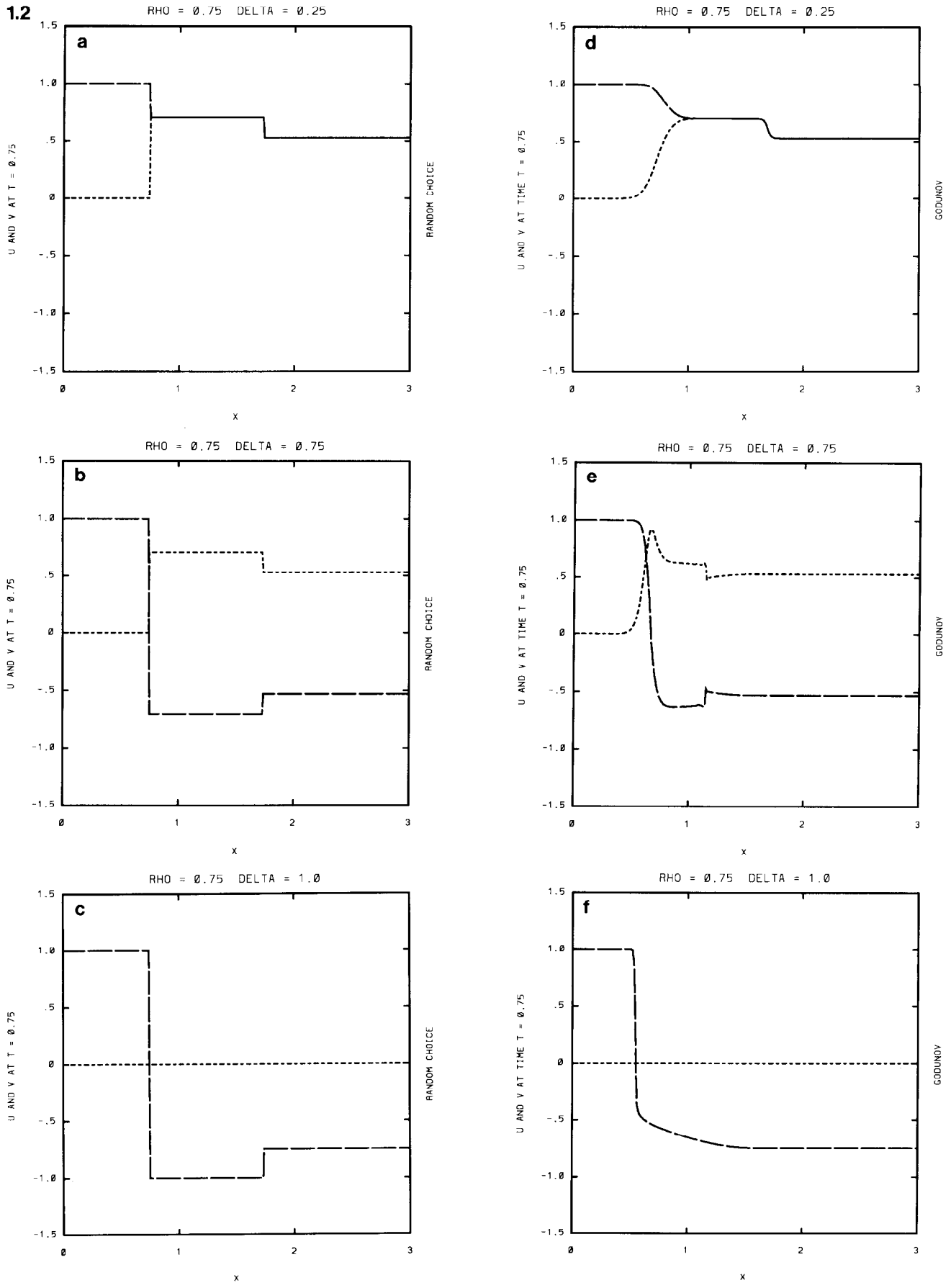

FIG. 1—*Continued*

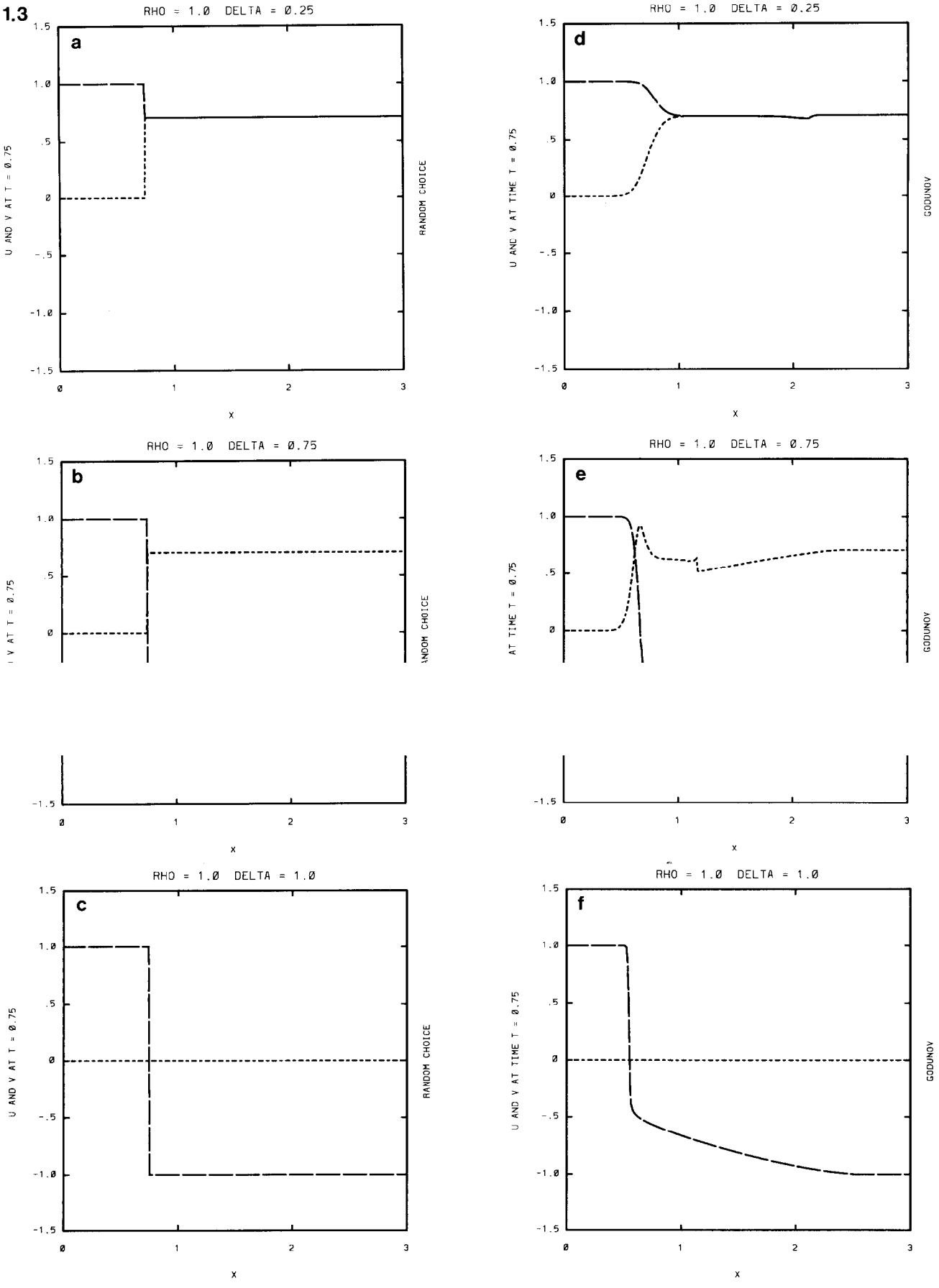

FIG. 1—*Continued*

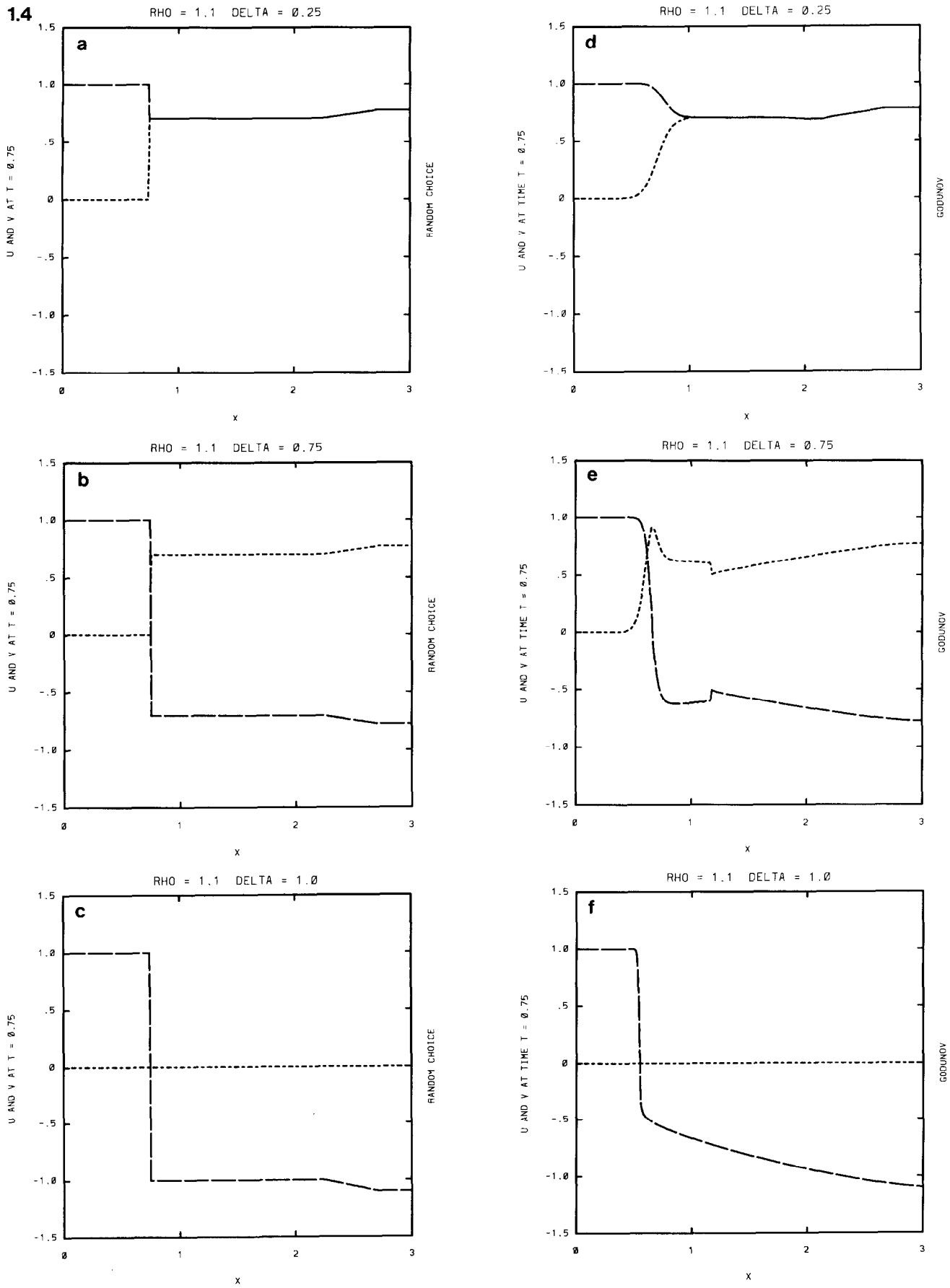

FIG. 1—*Continued*

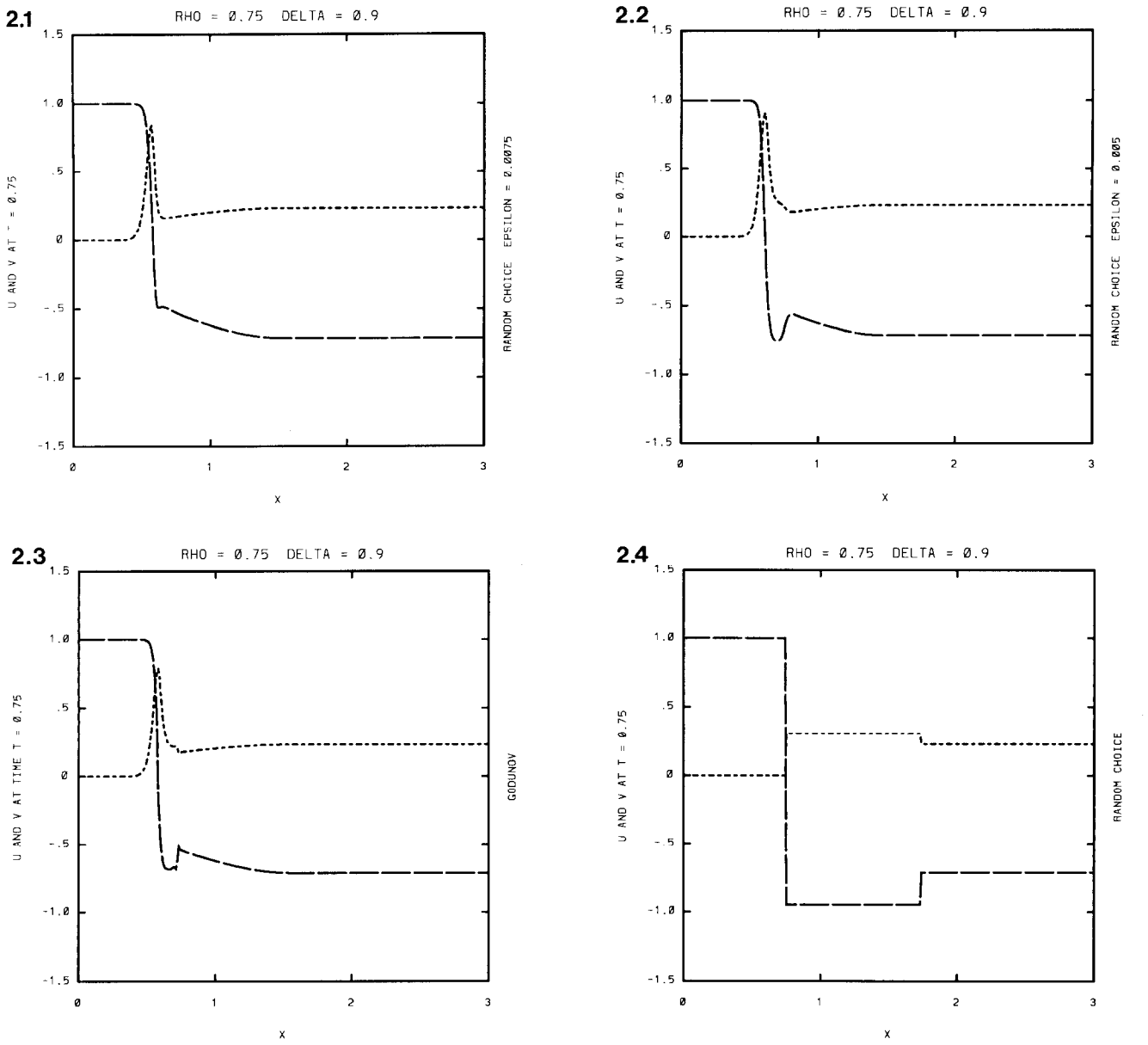

FIG. 2. A comparison of the Random Choice scheme, with various values of the viscosity parameter ε, and the Godunov scheme. For these plots, $\rho = 0.75$ and $\delta = 0.9\pi$. In Figure 2.1, $\varepsilon = 0.0075$; in Figure 2.2, $\varepsilon = 0.005$. Figure 2.3 shows results using the Godunov scheme. Figure 2.4 shows results from the inviscid Random Choice scheme, i.e., $\varepsilon = 0.0$.

For our numerical experiments, we discretized the interval $-0.15 \leqslant x \leqslant 3.0$. The Riemann data was of the form

$$U^0(x) = \begin{cases} U_l, & -0.15 < x < 0 \\ U_r, & 0 < x < 3.0 \end{cases}$$

with

$$U_l = (1, 0), \qquad U_r = (\rho \cos \delta, \rho \sin \delta) \tag{3.1}$$

and ρ and δ chosen from the values $\rho = 0.25, 0.75, 1.0, 1.1,$ and $\delta = 0.0, 0.25\pi, 0.75\pi, 0.9\pi, 0.95\pi, \pi$. Using each of the schemes described in Section 2.6, we computed the solutions up to time $t = 0.75$, which, with our x-interval, allows sufficient travel distance for all waves to separate. Computations were performed on a Sun SparcStation 1. To facilitate comparison of results, we always used the same space step $\Delta x = 0.01$, and the time step $\Delta t = 0.9\, \Delta x / \max(3\, |U^0|^2)$, i.e., 90% of the maximal value allowed by the CFL-condition. We emphasize that specifics of the issues we illustrate below

FIG. 3. The competition between dynamics and viscosity is illustrated in this sequence of plots, which shows the results of the Random Choice scheme with different values of viscosity and the Godunov scheme. In each plot, $\rho = 0.75$ and δ takes the values $0.75\pi, 0.95\pi, 1.0\pi$. In Figure 3.1, $\varepsilon = 0.0075$; in Figure 3.2, $\varepsilon = 0.005$. Figure 3.3 shows results using the Godunov scheme. Figure 3.4 shows results from the inviscid Random Choice scheme.

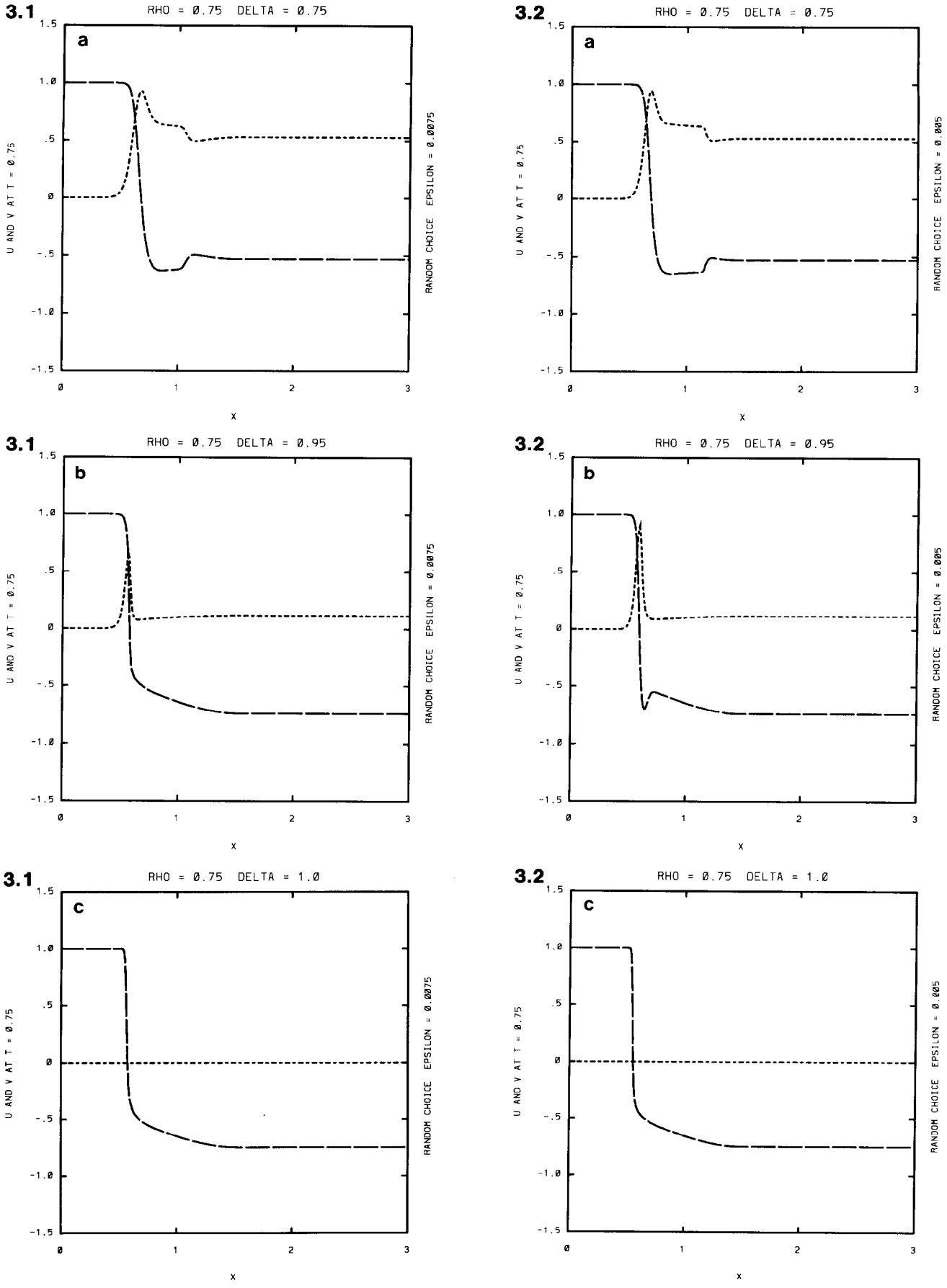

FIG. 3—*Continued*

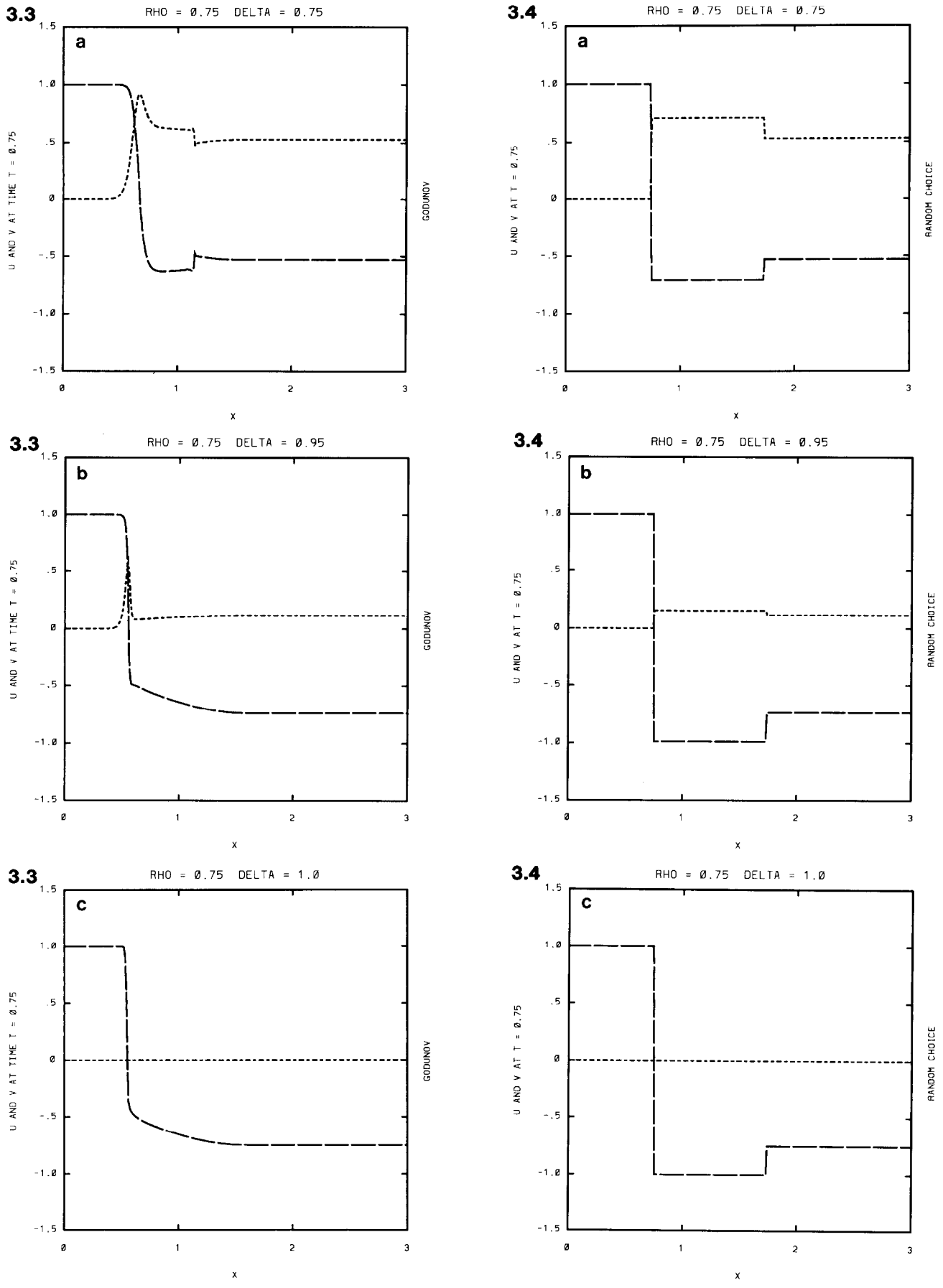

FIG. 3—*Continued*

are changed when the grid is refined, but all of the issues have counterparts on the refined grids. (Remark: The reader should recall that the size of artificial viscosity introduced in certain numerical schemes, as in (2.8), depends on space and time steps.)

We present a large selection of numerical results in order to address the following three topics: (a) a comparison between explicit resolution and implicit approximation of the wave pattern; (b) the strong dependence of solutions with special initial data on the size of artificial viscosity; (c) the subtle balance between the ideal dynamics and viscous effects for such data.

The results obtained by the two high-order Godunov schemes were always very similar, both qualitatively and quantitatively. Also the results from the first-order upwind scheme differed only slightly from these second-order methods. Thus we restrict our graphic display here to output from the random choice scheme, the Bell–Colella–Trangenstein second-order Godunov scheme and the combination of random choice with Crank–Nicholson.

To illustrate (a), the pictures in Fig. 1 show solutions obtained by random choice and the Godunov scheme, for the four values of ρ (Figs. 1.1–1.4), and $\delta = 0.25\pi,\ 0.75\pi,\ \pi$.

Aspect (b) is illustrated by the pictures in Fig. 2, which show solutions obtained by the various schemes. Figures 2.1 and 2.2 show the results of solving (2.9) as described with different values of ε. In Fig. 2.1, $\varepsilon = 0.0075$ (i.e., $\varepsilon = \frac{3}{4}\,\Delta x$); in Fig. 2.2, $\varepsilon = 0.005$ (i.e., $\frac{1}{2}\,\Delta x$). Figure 2.3 presents the results using the Godunov scheme. Figure 2.4 shows results using the random choice scheme. Data are given by (3.1) with $\rho = 0.75$, $\delta = 0.9\pi$.

Finally, topic (c) is made visible in the graphics of Fig. 3, which presents a sequence of data that approach the interesting case $\delta = \pi$. Shown are the results using: (Fig. 3.1), (2.9) with $\varepsilon = 0.0075$; (Fig. 3.2), Eq. (2.9) with $\varepsilon = 0.005$; (Fig. 3.3), second-order Godunov method; (Fig. 3.4), the random choice method. The data are given by $\delta = 0.75\pi,\ 0.95\pi,\ \pi$ with constant $\rho = 0.75$.

4. INTERPRETATION

In this section, we will try to elucidate the origin and meaning of the results from the numerical experiments presented in Section 3. Specifically, we will collect some analytical results on (1.1) (in Sub-section 4.1), discuss details of the individual experiments (in Sub-section 4.2), and give more details on the relationship of (1.1) to physical models (in Sub-section 4.3).

4.1. *Some Analytical Results*

We begin by examining more closely the "intuitive" way of solving the Riemann problem for (1.1) that was introduced at the very beginning of this paper. To any Riemann data (1.2), this approach assigns a solution $U(x, t) = \hat{U}(x/t)$ via:

if $|U_l| < |U_r|$,

$$\hat{U}(\sigma) = \begin{cases} U_l, & \sigma < |U_l|^2 \\ U_m, & |U_l|^2 < \sigma < 3\,|U_l|^2 \\ (\sigma/3)^{1/2}\, U_r/|U_r|, & 3\,|U_l|^2 < \sigma < 3\,|U_r|^2 \\ U_r, & \sigma > 3\,|U_r|^2, \end{cases} \tag{4.1.1}$$

if $|U_l| \geqslant |U_r|$,

$$\hat{U}(\sigma) = \begin{cases} U_l, & \sigma < |U_l|^2 \\ U_m, & |U_l|^2 < \sigma < |U_l|^2 + |U_l|\,|U_r| + |U_r|^2 \\ U_r, & \sigma > |U_l|^2 + |U_l|\,|U_r| + |U_r|^2, \end{cases} \tag{4.1.2}$$

with $U_m = (|U_l|/|U_r|)\,U_r$ in both cases. Denoting by $S(U^0)$ the solution thus assigned to data U^0, we have the following property, [14]:

LEMMA 1. (Dynamical stability.) *S is continuous with respect to the $\mathscr{L}^1_{\text{loc}}$-topology. Discontinuities are stable against small perturbations.*

For the general Cauchy problem, we have:

LEMMA 2. (i) *Let U^0 be any initial data for* (1.1) *such that the total variation of $r \circ U^0$ and $\theta \circ U^0$ is bounded. Then, for any pair $(\Delta x, \Delta t)$ satisfying the Courant–Friedrichs–Lewy condition, $3 \sup |U^0|^2\, \Delta t \leqslant \Delta x$, using the solution operator S for the Riemann problem of* (1.1) *in Glimm's scheme defines an approximate solution $\tilde{U} = \tilde{U}(x, t)$ for all $x \in \mathbb{R}$, $t \geqslant 0$. If ${}^k(\Delta x, \Delta t)$ is an appropriate sequence of such pairs converging to zero, the corresponding sequence of approximants ${}^k\tilde{U}$ contains a subsequence which converges to a weak solution of* (1.1). (ii) *The limit in* (i) *is the unique weak solution in a certain natural function space and depends $\mathscr{L}^1_{\text{loc}}$-continuously on the data.*

In [36], Liu and Wang have proved statements analogous to (i) for a class of rotationally invariant systems under certain assumptions; only slight modifications are required to extend their proof to (i). (ii) follows from [15].

Next, we examine the solution operator for the Riemann problem of (1.3) given by [32, 45]. To any data

$$u^0 = \begin{cases} u_l, & x < 0 \\ u_r, & x > 0, \end{cases} \tag{4.2}$$

this solution operator assigns a function $u(x, t) = \hat{u}(x/t)$ as follows:

if $u_l \in [0, 1]\, u_r$,

$$\hat{u}(\sigma) = \begin{cases} u_l, & \sigma < 3u_l^2 \\ (\sigma/3)^{1/2}\, u_r/|u_r|, & 3u_l^2 < \sigma < 3u_r^2 \\ u_r, & \sigma > 3u_r^2; \end{cases} \tag{4.3.1}$$

if $u_r \in [-\frac{1}{2}, 1]\, u_l$,

$$\hat{u}(\sigma) = \begin{cases} u_l, & \sigma < u_l^2 + u_l u_r + u_r^2 \\ u_r, & \sigma > u_l^2 + u_l u_r + u_r^2; \end{cases} \tag{4.3.2}$$

if $u_r \in (-\infty, -\frac{1}{2})\, u_l$,

$$\hat{u}(\sigma) = \begin{cases} u_l, & \sigma < \frac{3}{4}u_l^2 \\ (\sigma/3)^{1/2}\, u_r/|u_r|, & \frac{3}{4}u_l^2 < \sigma < 3u_r^2 \\ u_r, & \sigma > 3u_r^2. \end{cases} \tag{4.3.3}$$

Denoting by $s(u^0)$ the solution u thus assigned to given data u^0, we characterize this procedure as follows:

LEMMA 3. (i) (Dynamical stability.) *s is continuous with respect to the $\mathscr{L}^1_{\text{loc}}$-topology. Discontinuities are stable against small perturbations.* (ii) (Vanishing viscosity.) *For given data u^0, $s(u^0)$ is the unique limit obtained by the vanishing viscosity method.*

These statements follow from Kruskov's theory, [29]. By rotational invariance, (1.3) represents the restriction of (1.1) to any line (in phase space) through the origin. Thus s may be lifted in an obvious manner to yield a solution operator for the Riemann problem of (1.1) with co-linear data. The difficulty with the vanishing viscosity approach for (1.1) is now apparent; solutions obtained from s are different from those obtained from S for data such that $0 \in (U_l, U_r)$. The following discrepancy has been proved in [14]:

LEMMA 4. (Vanishing viscosity.) *If, for* (1.1) *with given data* (1.2), *the vanishing viscosity method converges to a piecewise continuous self-similar wave pattern, then this limit is $S(U^0)$ whenever $0 \notin (U_l, U_r)$. If, however, $0 \in (U_l, U_r)$, then the solution of the viscous problem* ((2.9) *with* (1.2)) *converges to the solution corresponding to s.*

This shows that (1.1) and (2.9) are not uniformly close to each other.

4.2. *Details of the Experiments*

Due to the similarity properties of system (1.1), all families of solutions to the Riemann problem corresponding to different given values of $U_l \neq 0$ are isomorphic to each other in the sense that a one-to-one correspondence between members of any two such families is established by an appropriately chosen scaling transformation. Thus, data (3.1) cover all cases with $U_l \neq 0$. In picking interesting values of ρ we were guided by the fact that the structure of the solution $S(U^0)$ undergoes a change at $\rho = 1$; specifically, the fast wave in $S(U^0)$ is a shock for $\rho < 1$, but a rarefaction for $\rho > 1$. Similarly, at $\delta = \pi$ the structure of the solution obtained by lifting $s(u^0)$ changes at $\rho = 0.5$; $s(u^0)$ changes from a single shock, for $\rho < 0.5$, to a composite wave, i.e., a shock with contact to an adjacent rarefaction wave, for $\rho > 0.5$. These exact solutions may be read off immediately from (4.1) and (4.3).

The results plotted in Fig. 1 show that for small δ there is a reasonable agreement between the solutions obtained from the random choice method and those computed by using the Godunov scheme (modulo the spreading of contact discontinuities by the latter). On the other hand, when $\delta \to \pi$, there is a marked difference between the two.

We claim that this discrepancy is fully explained by the singular behavior of the vanishing viscosity approach observed in Lemma 4. The validity of this claim becomes apparent if we view the Godunov scheme as an approximation to a viscous regularization of (1.1) rather than to (1.1) itself. To test this explanation, we examined the influence of artificial viscosity by solving (2.9). Hence the plots in Fig. 2. Note that, according to Lemma 4, the singular behavior occurs for data with $0 \in (U_l, U_r)$ (or nearly so), corresponding to $\delta \approx \pi$; this is why we picked the value $\delta = 0.9\pi$ for this series of pictures. From the pictures it is obvious that, for fixed data, reducing the amount of artificial viscosity introduced by the scheme results in closer agreement with the ideal solution obtained from S.

Let us consider a family of data

$$U_l = (1, 0),$$
$$U_r = (\rho \cos \delta, \rho \sin \delta) \qquad \text{with} \quad \rho > 0 \quad \text{fixed} \quad \text{and} \quad \delta \approx \pi. \tag{4.4}$$

Assume that there exist reasonably behaved solutions $U_{\varepsilon,\delta}$ of the regularization (2.9) for data (4.4). For a fixed value of $\varepsilon > 0$ one expects $U_{\varepsilon,\delta}$ to tend to $U_{\varepsilon,\pi}$ for $\delta \to \pi$; as a consequence of (ii) of Lemma 3, $U_{\varepsilon,\pi}$ will not differ much from the composite wave solution obtained from s if ε is small. On the other hand, if $\delta \neq \pi$ is kept fixed, Lemma 4 suggests that $U_{\varepsilon,\delta}$ converge, with $\varepsilon \downarrow 0$, to the dynamically stable solution obtained from S. Thus, there must be a subtle competition between dissipation (ε) and dynamics (δ). This is what our third series of plots, in Fig. 3, is about. From top to bottom, δ tends to π; proceeding from Fig. 3.1 to Fig. 3.4, the dissipation is decreased until it vanishes in Fig. 3.4. The pictures clearly illustrate the competition between dynamics and viscosity.

We summarize our findings in the following

Conclusion. The Riemann problem for the hyperbolic system (1.1) is well posed. It makes sense to use its dynamically stable solution, given by (4.1), in the random choice scheme; applying this scheme to Riemann data yields the

dynamically stable solution. Using other standard schemes for the Riemann problem of (1.1) shows that this solution is well approximated by the solution of the corresponding viscous problem (2.9) for any fixed small values ε of the viscosity, as long as the data U_l, U_r are not too close (depending on ε) to satisfying the condition $0 \in (U_l, U_r)$. On one hand, as the data come to meet this condition more closely, the dynamically stable solution ceases to resemble the solution of the viscous problem. On the other hand, as ε is decreased, the region (in (U_l, U_r)-space) of good agreement expands, ultimately (for $\varepsilon \approx 0$) covering all data for which $0 \notin (U_l, U_r)$.

4.3. *On the Relationship to Physical Models*

The system (1.1) considered in this paper is an example from the class of systems characterized by a rotationally equivariant flux, i.e.,

$$f(U) = \Phi(|U|^2)\, U. \tag{4.6}$$

Systems of this kind were considered by Keyfitz and Kranzer in [28], who were interested in the Riemann problem for the equations governing planar motions of an ideal elastic string. These equations are of the form (see Antman [1])

$$\begin{aligned} U_t - V_x &= 0 \\ V_t - f(U)_x &= 0 \end{aligned} \tag{4.7}$$

with f satisfying (4.6). Any system exhibiting the structure (4.7) is hyperbolic if the corresponding system

$$U_t + f(U)_x = 0 \tag{4.8}$$

is hyperbolic and the eigenvalues of Df are all positive. Moreover, there is an intimate relationship between the centered solutions of (4.7) and (4.8). This is why Keyfitz and Kranzer studied the Riemann problem for (4.8) with (4.6) first, with Φ satisfying certain assumptions. In doing so, they proved a number of interesting properties. Following these lines, Shearer [42] proved unique solvability of the original problem. Nonlinear plane waves in incompressible isotropic elastic bodies are also governed by equations of the form (4.7) with symmetry (4.6) [2].

The equations for nonlinear plane waves in compressible isotropic hyperelastic media have the form (4.7) [9] and so do the equations governing nonlinear plane magnetohydrodynamic waves [11]. In these two cases, the function f has a rotational equivariance which is not precisely of the form (4.6).

In all these cases, the behavior of certain transverse components of the state variable is adequately modeled (in a certain sense) by (4.8) with a flux (4.6). Obviously, the leading (nonlinear) part in a Taylor expansion of any such flux at $U = 0$ is, up to a multiplicative constant, $|U|^2 U$. This is what makes (1.1) a significant model [4, 12]. (Remark: This small amplitude expansion argument does not apply to the elastic string problem, the setting which first gave rise to a study of the Riemann problem for a system with rotationally equivariant flux. In this problem, U represents the derivative of particle position along the string; hence U cannot vanish, since $U = 0$ would correspond to an infinite shrinking of the string. One must restrict phase space away from this unphysical value. More generally, the elastic string problem cannot be hyperbolic for $|U| < 1$; see Carasso, Rascle, and Serre [6].) With the exception of the elastic string problem, small values of $|U|$ do make sense for all systems mentioned above.

In particular, small values of $|U|$ arise in magnetohydrodynamics. With respect to this field of application, the work of Brio and Wu [5] and Wu [46] has been pioneering. They have investigated the so-called intermediate shocks. Brio and Wu contend that these shocks are physical and support this claim by numerical computations. In a sense our work may be considered as providing further evidence for this claim since the shocks appearing in the composite solution to the restricted problem (1.3) correspond to (certain) intermediate MHD shocks. On the other hand, our experiments also restrict this claim considerably. Let us explain this statement. As viscosity decreases ("viscosity" corresponds to electrical resistivity in this setting), ever smaller perturbations of the data split the intermediate shock into the dynamically stable two-dimensional wave pattern of a contact discontinuity plus another wave. In the inviscid limit, intermediate shocks are completely unstable against generic perturbations.

The model character of system (1.1) allows us to restate the conclusion drawn in the preceding sub-section as a rule for the construction of good numerical schemes for generic rotationally degenerate systems of physical conservation laws, valid at least in the region corresponding to small values of U: As long as discontinuities of a certain type (satisfying an analogue of the above condition $0 \in (U_l, U_r)$) do not form, the presence or absence of a small viscosity plays no important rôle in determining the physical solution. When such discontinuities do occur, one must make a clear distinction between the ideal and the viscous problem, and take care that the viscosity introduced by the computational method correctly models the desired (zero or non-zero) physical viscosity.

ACKNOWLEDGMENT

We would like to thank M. Brio for stimulating discussions and J. Fehribach for helpful comments on the random choice scheme. This research began while the authors were Visiting Members at the Institute for Mathematics and its Applications, with support provided by the NSF and

ONR through grants to the IMA and the Minnesota Supercomputer Institute. The authors would like to thank the IMA and its staff for assistance and hospitality.

REFERENCES

1. S. Antman, *Am. Math. Soc. Monthly* **87**, 359 (1980).
2. S. Antman and Z.-H. Guo, *J. Elast.* **14**, 249 (1984).
3. J. Bell, P. Colella, and J. Trangenstein, *J. Comput. Phys.* **82**, 362 (1989).
4. M. Brio and J. Hunter, *Commun. Pure Appl. Math.* **43**, 1037 (1990).
5. M. Brio and C. C. Wu, *J. Comput. Phys.* **75**, 400 (1988).
6. C. Carasso, M. Rascle, and D. Serre, *Math. Mod. Numer. Anal.* **19**, 573 (1985).
7. R. H. Cohen and R. M. Kulsrud, *Phys. Fluids* **17**, 2215 (1974).
8. P. Colella, *SIAM J. Sci. Statist. Comput.* **3**, 76 (1982).
9. C. M. Dafermos, in *Trends in Applications of Pure Mathematics to Mechanics*, Vol. III, edited by R. J. Knops (Pitman, London, 1981), p. 96.
10. J. D. Fehribach and M. Shearer, *Appl. Anal.* **32**, 1 (1989).
11. H. Freistühler, *Arch. Rational Mech. Anal.* **113**, 39 (1991).
12. H. Freistühler, in *Nonlinear Hyperbolic Equations, Theory, Computational Methods and Applications*, edited by J. Ballmann and R. Jeltsch (Vieweg, Braunschweig, 1989), p. 149.
13. H. Freistühler, *J. Differential Eqs.* **87**, 205 (1990).
14. H. Freistühler, Dynamical stability and vanishing viscosity: A case study of a non-strictly hyperbolic system, *Commun. Pure Appl. Math.*, to appear.
15. H. Freistühler, On the Cauchy problem for a class of hyperbolic systems of conservation laws, *J. Differential Eqs.*, submitted.
16. H. Freistühler, On the stability of intermediate magnetohydrodynamic shocks, *J. Geophys. Res.* **96**, 3382 (1991).
17. H. Freistühler and E. B. Pitman, A numerical study of a rotationally degenerate hyperbolic system. Part II. The Cauchy problem, in preparation.
18. H. Freistühler and E. B. Pitman, A numerical study of a rotationally degenerate hyperbolic system. Part III. Adding viscosity, in preparation.
19. H. Gilquin and D. Serre, rapport de recherche no. 0 (Laboratoire de Mathématiques Ecole Normale Supérieure de Lyon, Lyon, 1988).
20. J. Glimm, *Commun. Pure Appl. Math.* **18**, 95 (1965).
21. J. Glimm, in *Nonlinear Hyperbolic Equations, Theory, Computational Methods and Applications*, edited by J. Ballmann and R. Jeltsch (Vieweg, Braunschweig, 1989), p. 169.
22. S. K. Godunov, *Math. Sb.* **47**, 271 (1959).
23. V. V. Gogosov, *J. Appl. Math. Mech.* **25**, 148 (1961).
24. A. Harten, P. Lax, and B. van Leer, *SIAM Rev.* **25**, 357 (1983).
25. E. Isaacson, Global solution of a Riemann problem for a non-strictly hyperbolic system of conservation laws arising in enhanced oil recovery, Rockefeller University preprint, 1978 (unpublished).
26. E. Isaacson, D. Marchesin, B. Plohr, and B. Temple, *SIAM J. Appl. Math.* **48**, 357 (1988).
27. C. F. Kennel, R. D. Blandford, and C. C. Wu, *Phys. Fluids B* **2**, 253 (1990).
28. B. Keyfitz and H. Kranzer, *Arch. Rational Mech. Anal.* **72**, 219 (1980).
29. S. Kruskov, *Math. Sb.* **123**, 228 (1970); Eng. transl., *Math. USSR Sb.* **10**, 217 (1970).
30. P. D. Lax, *Commun. Pure Appl. Math.* **10**, 537 (1957).
31. B. van Leer, *J. Comput. Phys.* **37**, 101 (1979).
32. T.-P. Liu, *J. Differential Eqs.* **18**, 218 (1975).
33. T.-P. Liu, *Commun. Math. Phys.* **57**, 135 (1977).
34. T.-P. Liu, Amer. Math. Soc. Memoirs, Vol. 240 (Amer. Math. Soc., Providence, RI, 1981).
35. T.-P. Liu, On the viscosity criterion for hyperbolic conservation laws, in *Viscous Profiles and Numerical Methods for Shockwaves*, edited by M. Shearer (SIAM, Philadelphia, 1991), p. 105.
36. T.-P. Liu and J. Wang, *J. Differential Eqs.* **57**, 1 (1985).
37. A. Majda and R. Pego, *J. Differential Eqs.* **56**, 229 (1985).
38. O. A. Oleinik, *Usp. Mat. Nauk* **12**, 3 (1957); Engl. transl., *Am. Math. Soc. Transl. Ser. 2* **26**, 95 (1963).
39. P. Roe, *J. Comput. Phys.* **43**, 357 (1981).
40. D. G. Schaeffer, *Adv. Math.* **11**, 368 (1973).
41. D. G. Schaeffer, M. Shearer, D. Marchesin, and P. Paes-Leme, *Arch. Rational Mech. Anal.* **97**, 299 (1987).
42. M. Shearer, *J. Differential Eqs.* **61**, 149 (1986).
43. R. J. Tait and K. Abdella, *Longitudinal Waves in a Finite Nonlinear Elastic String*, University of Alberta preprint 1989 (unpublished).
44. B. Temple, *Adv. Appl. Math.* **3**, 335 (1982).
45. B. Wendroff, *J. Math. Anal. Appl.* **38**, 640 (1972).
46. C. C. Wu, *Geophys. Res. Lett.* **14**, 668 (1987).